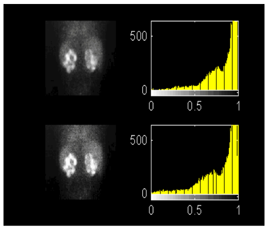

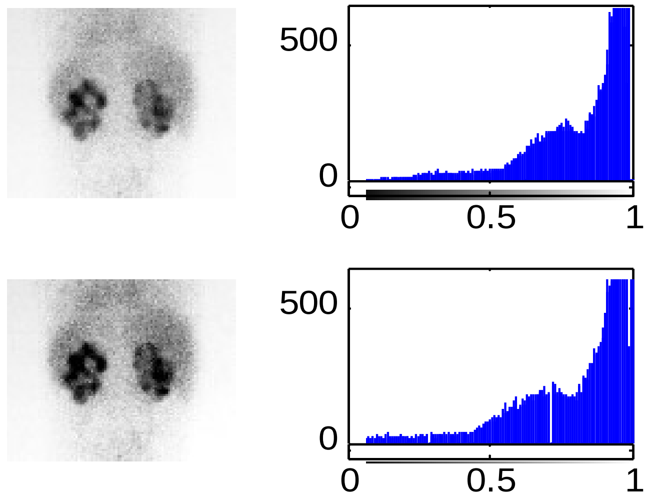
500
0
0
0.5
1
500
0
0
0.5
1

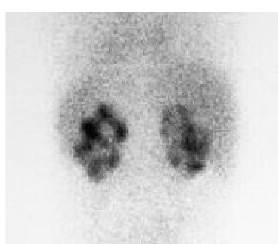

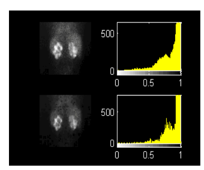

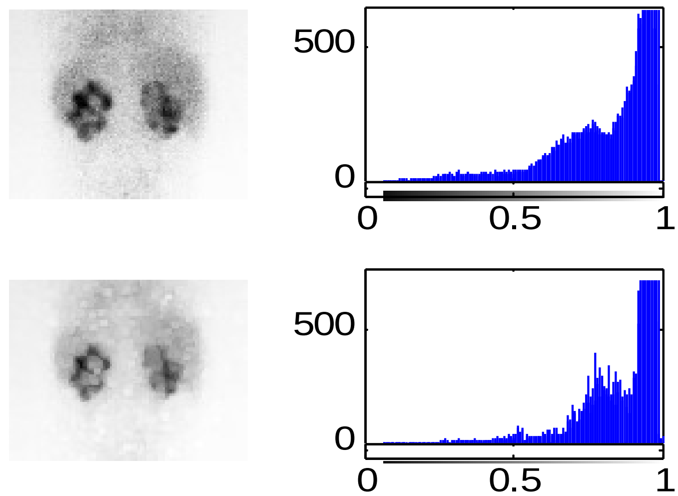
500
0
0
0.5
1
500
0
0
0.5
1

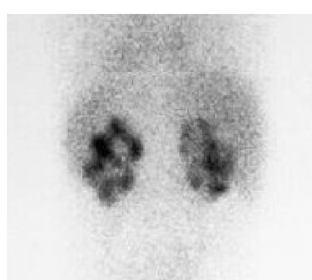

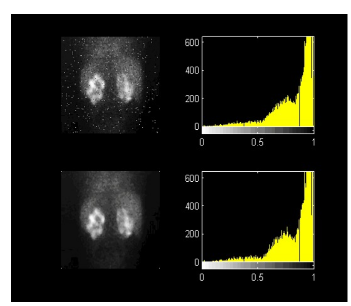
600
400
200
0
0
0.5
1
600
400
200
0
0
0.5
1

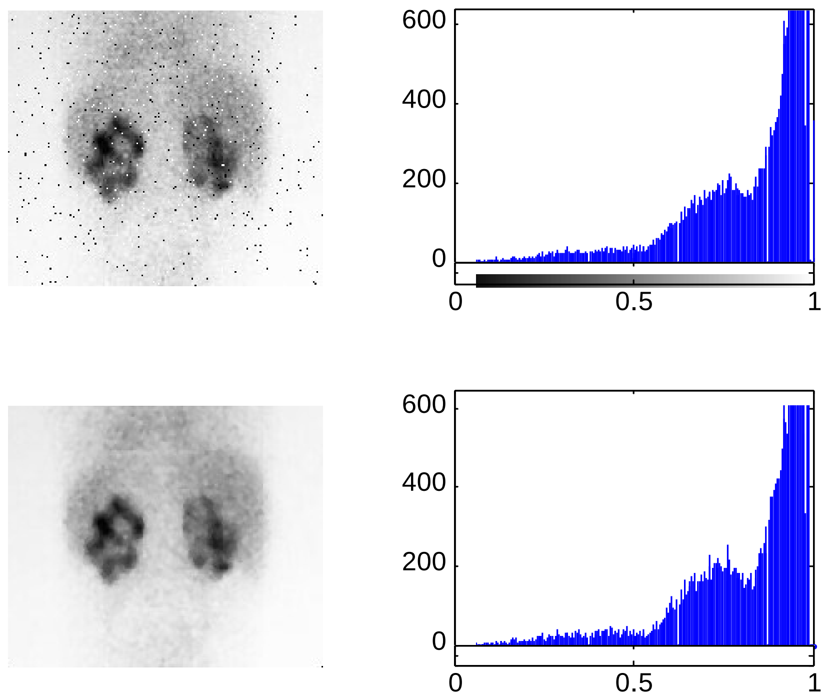
600
400
200
0
0
0.5
1
600
400
200
0
0
0.5
1

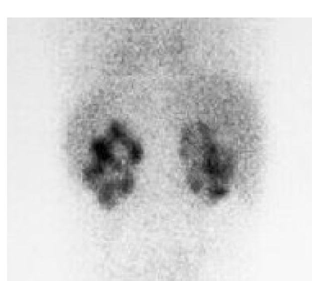

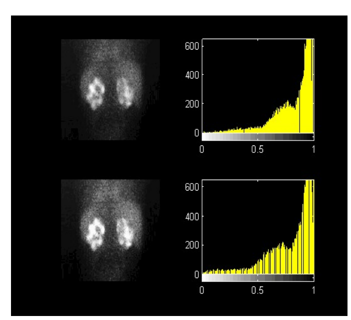

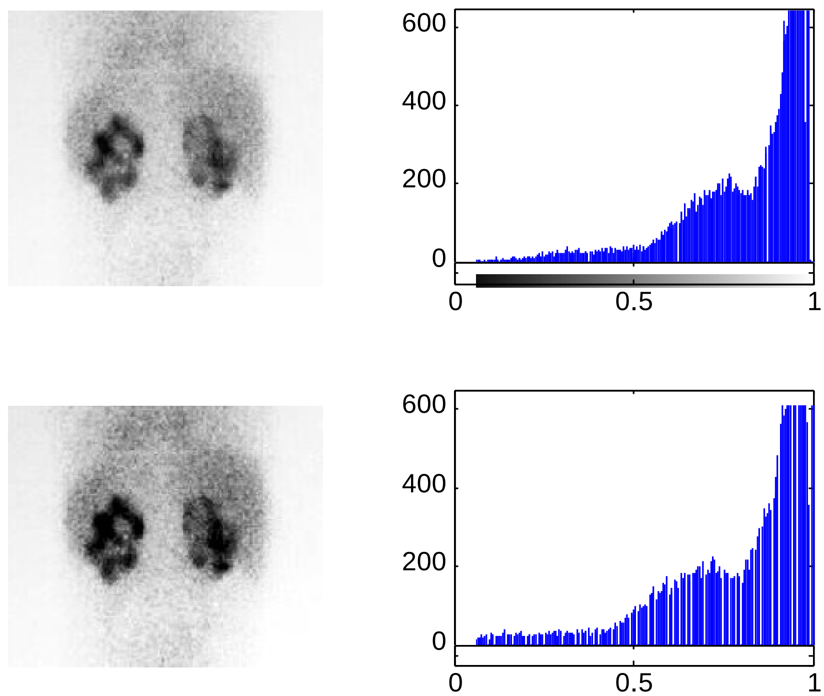
600
400
200
0
0
0.5
1
600
400
200
0
0
0.5
1

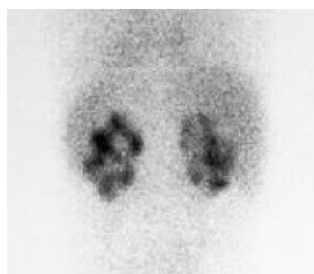

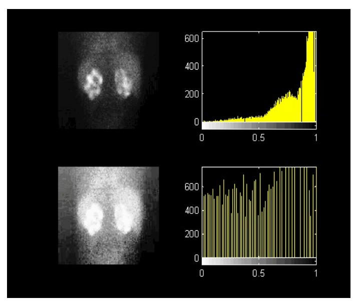

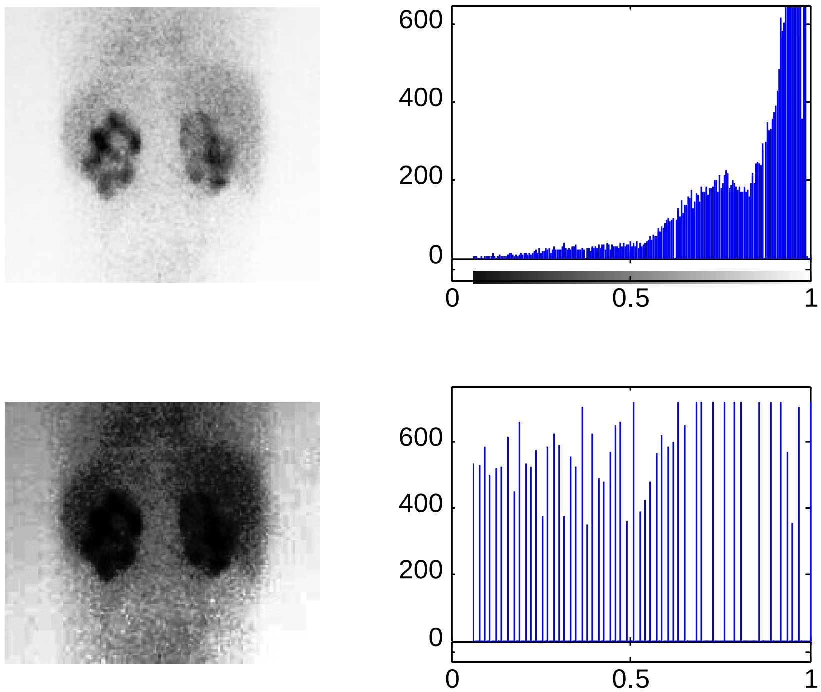
600
400
200
0
0
0.5
1
600
400
200
0
0
0.5
1

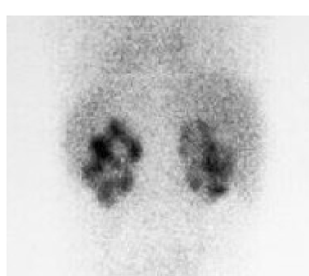

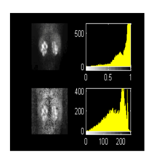

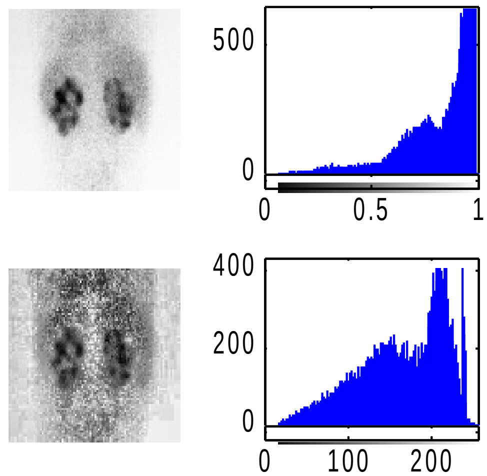
500
0
0
0.5
1
400
200
0
0
100
200

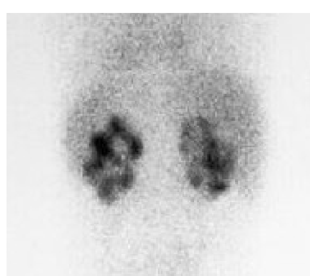

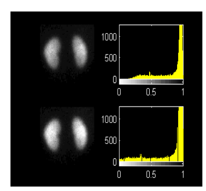
1000
500
0
0
0.5
1
1000
500
0
0
0.5
1

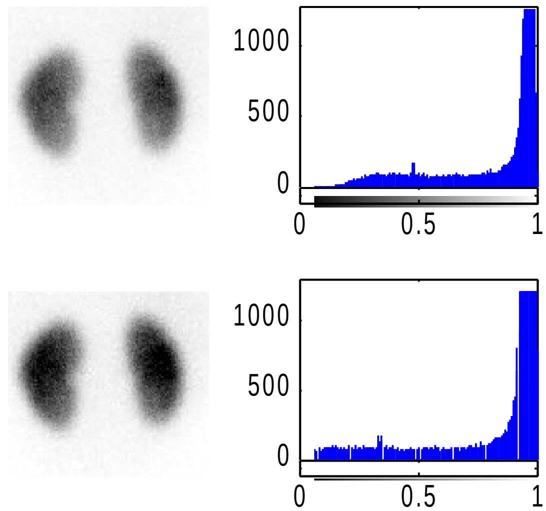
1000
500
0
0
0.5
1
1000
500
0
0
0.5
1

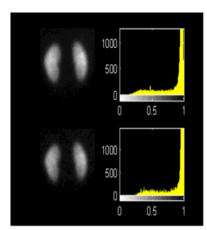
1000
500
0
0
0.5
1
1000
500
0
0
0.5
1

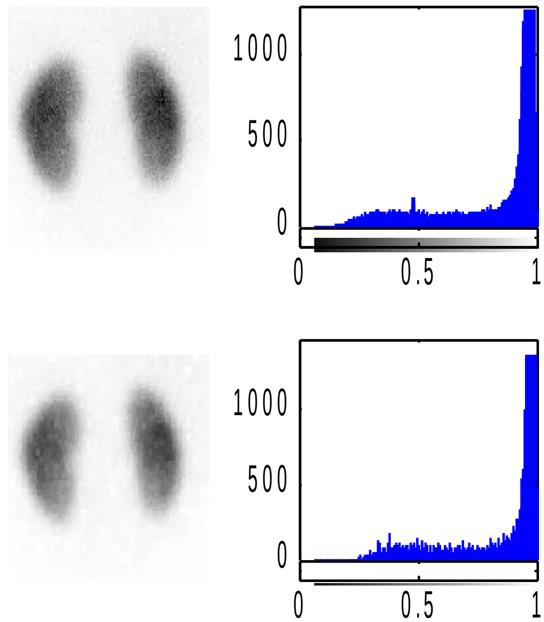
1000
500
0
0
0.5
1
1000
500
0
0
0.5
1

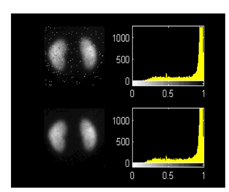

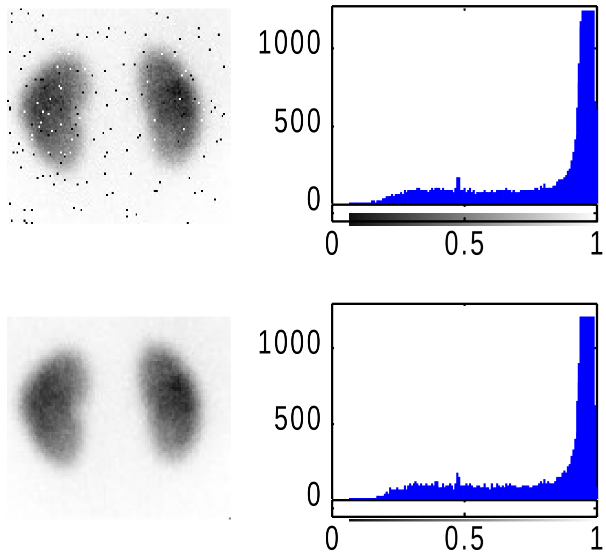
1000
500
0
0
0.5
1
1000
500
0
0
0.5
1

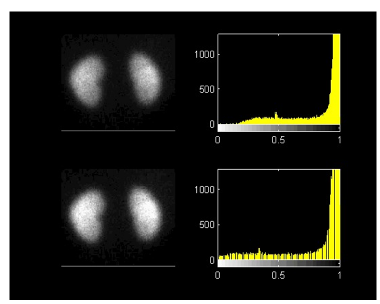
1000
500
0
0
0.5
1
1000
500
0
0
0.5
1

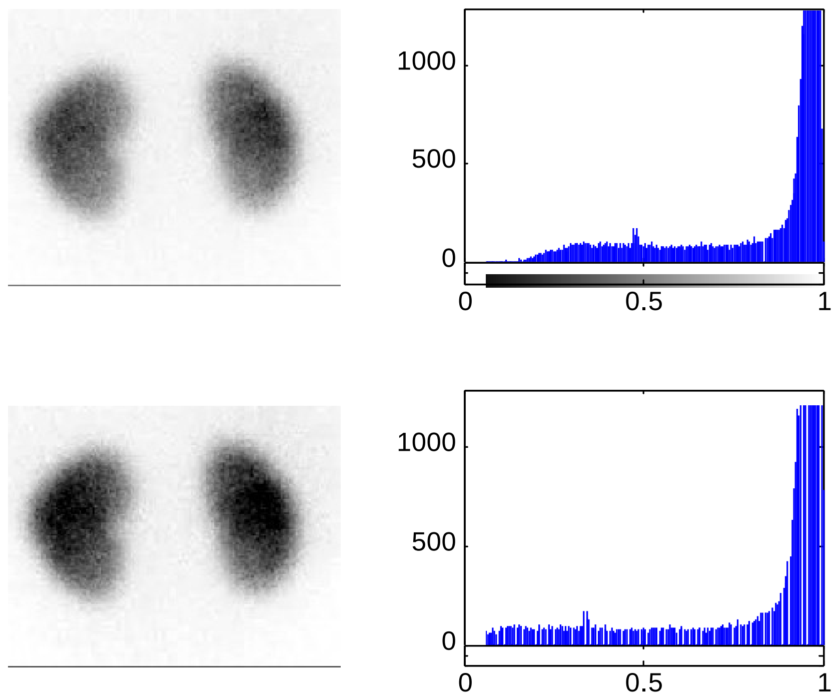
1000
500
0
0
0.5
1
1000
500
0
0
0.5
1

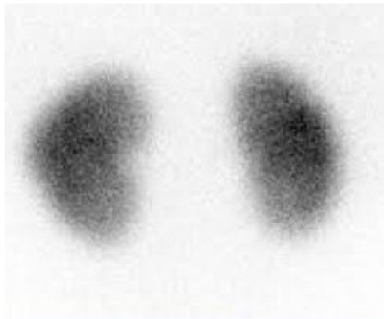

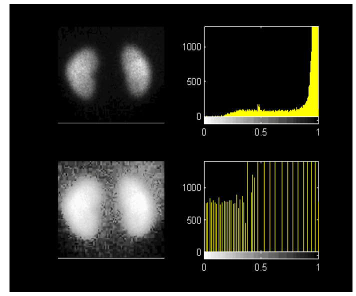
1000
500
0
0
0.5
1
1000
500
0
0
0.5
1

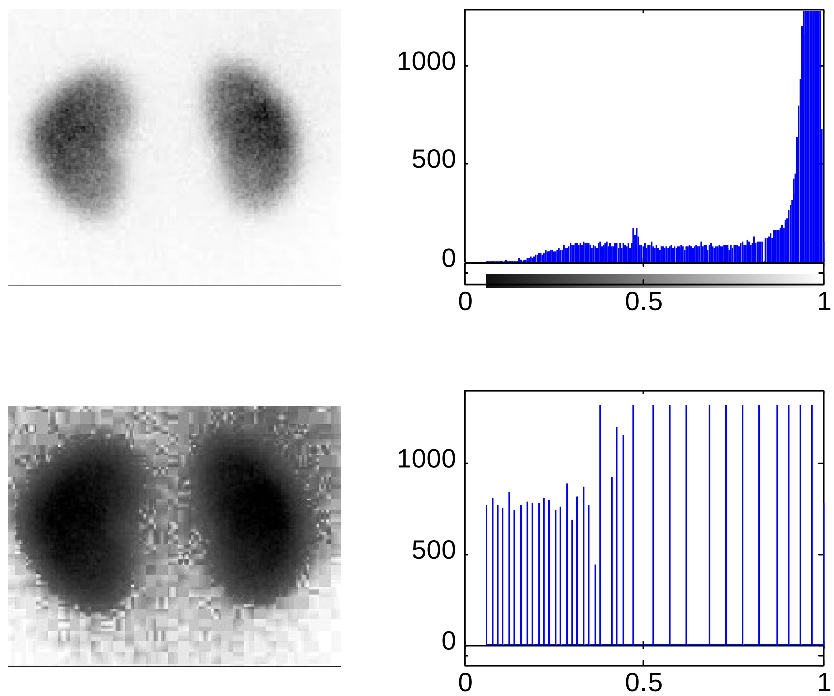
1000
500
0
0
0.5
1
1000
500
0
0
0.5
1

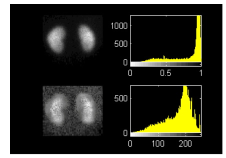
1000
500
0
0
0.5
1
500
0
0
100
200

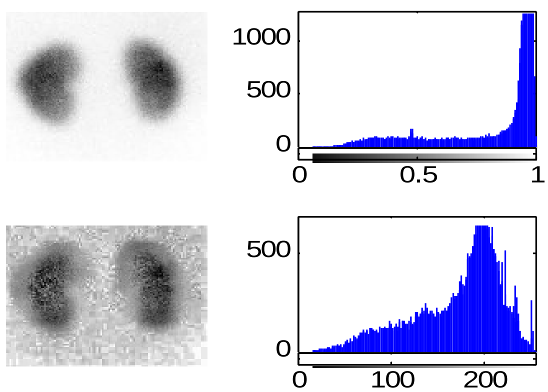
1000
500
0
0
0.5
1
500
0
0
100
200

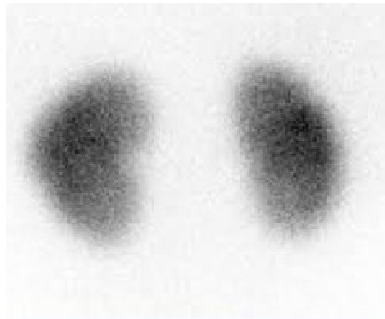


1
2
FORTE
FORTE

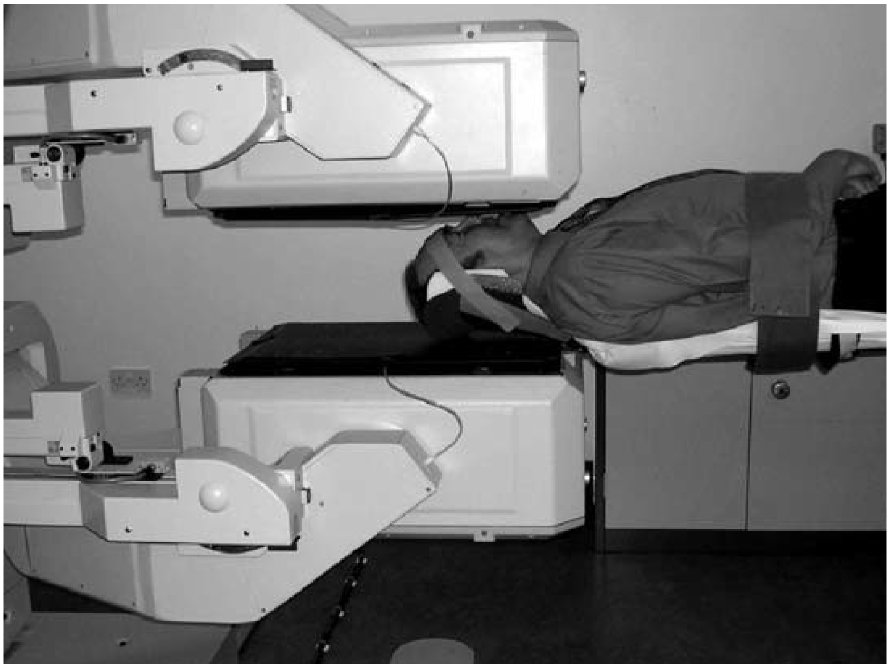

Chapter

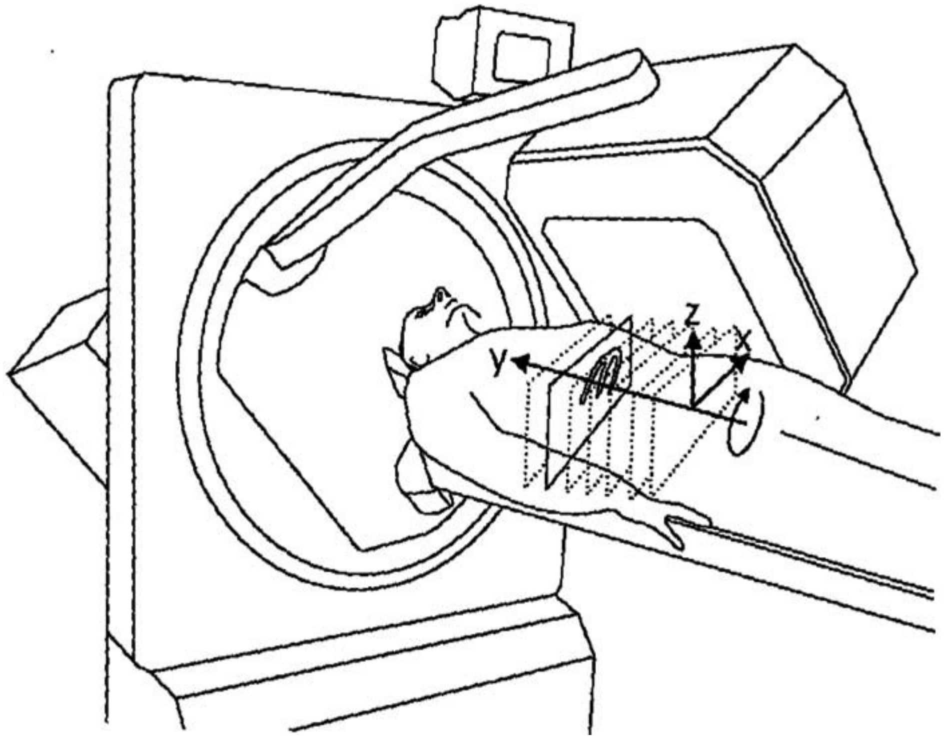

One

Introduction

1.1. Introduction:

The objective of a quality control programme of the gamma camera is to assure that the findings in the patient examination have their origin in the patient and not in the gamma camera itself. In such a complex system as a modern gamma camera there are many factors that contribute to the final image quality and if not kept under control they will result in a misinterpretation of the examination in terms of false positive or false negative results. A thorough evaluation of the gamma camera system at installation, and a comprehensive routine quality control programme, will guarantee reliable function and detect the majority of problems that can occur. Another important factor in a quality control programme is the nuclear medicine specialists and the technologists ability to recognize the types of artifacts that will occur in the images due to improper function of the equipment. A system of communication and reporting is fundamental, and the medical physicist has a key position in this. Advanced techniques of image processing and analysis find widespread use in medicine. In medical applications, image data are used to gather details regarding the process of patient imaging whether it is a disease process or a physiological process. Information provided by medical images has become a vital part of today's patient care. The images generated in medical applications are complex and vary notably from application to application. Nuclear medicine images show characteristic information about the physiological properties of the structures-organs. In order to have high quality medical images for reliable diagnosis, the processing of image is necessary. The scope of image processing and analysis applied to medical applications is to improve the quality of the acquired image and extract quantitative information from medical image data in an efficient and accurate way.

MatLab (Matrix Laboratory) is a high performance interactive software package for scientific and engineering computation developed by MathWorks (Mathworks Inc., 2009). MatLab allows matrix computation, implementation of algorithms, simulation, plotting of functions and data, signal and image processing by the Image Processing Toolbox. It enables quantitative analysis and visualisation of nuclear medical images of several modalities, such as Single Photon Emission Computed Tomography (SPECT), Positron Emission Tomography (PET) or a hybrid system (SPECT/CT) where a Computed Tomography system (CT) is incorporated to the SPECT system.The Image Processing Toolbox (Mathworks Inc., 2009) is a comprehensive set of reference-standard algorithms and graphical tools for image processing, analysis, visualisation and algorithm development. The measurement of gamma-camera linearity and resolution forms an important part of acceptance testing and routine quality control. Conventional techniques for measuring locations and widths of line spread functions require high precision digitization, usually via external analogue to digital converters. A technique is described for accurate measurement of peak location and width using coarsely sampled line spread functions. Results obtained for both simulated and actual gamma-camera data demonstrate that the method is capable of measuring peak deviations as small as 0.2 mm when the sampling interval is 1.5 mm or more. The precision of the method was found to be at least as good as conventional techniques. It is suggested that using the method accurate measurements of linearity can be made from a conventional 256*256 nuclear medicine image of a slit mask, and this enables routine evaluation of an important parameter of camera performance.

1.2. Problem of the study

Performance test is inaccurace may lead mislocation of certein point. Quality control is essential to check the quality image. Medical images are often deteriorated by noise due to various of interference and other factor associated with imaging process and data acquisition system. Radiation is a major risk in diagnostic in medical image. The problem is caused from overdose during the diagnosis due to improve the image.

1.3. Objectives

The main objective of this study was to enhance nuclear medicine images of kidneys using Filtering Technique.

1.3.1.Specific objectives

- To enhance of Nuclear Medicine Images of kidneys by using MatLab global and local enhancement techniques

- To evaluate contrast enhancement pattern in different panoramic images such as grey color.

-To evaluate the usage of new nonlinear approach for contrast enhancement of soft tissues in panoramic images.

1.4. Overview of study:

This study falls into five chapters, Chapter one, which is an introduction, deals with theoretical frame work of the study. It presents the statement of the of the study problems, objectives of the study, chapter two, deals with SPECT machine components and Q.C of SPECT (literature review). Chapter three deal with material and method, Chapter fours deals with (results) data presentation. Chapter five discusses the data (discussion), conclusion , recommendations and references.

Chapter Two

Literature Review

2.1. SPECT machine

Single-photon emission computed tomography (SPECT, or less commonly, SPET) is a nuclear medicine tomographic imaging technique using gamma rays . It is very similar to conventional nuclear medicine planar imaging using a gamma camera. However, it is able to provide true 3D information. This information is typically presented as cross-sectional slices through the patient, but can be freely reformatted or manipulated as required. SPECT imaging can be performed with any in vivo nuclear medicine radiotracer given the proper collimation for the chosen isotope and software for collection and processing of data. They are performed by acquiring a series of planar images and reconstructing the images into planes (angles), e.g., transverse, coronal, and sagittal (Pete Shackett et al, 2012).

This SPECT technique uses a gamma camera to record images at a series of angles around the patient. These images are then subjected to a form of digital image processing called Image Reconstruction in order to compute images of slices through the patient. (Kieran et al, 1996).

2.2.Basic principles:

The basic principle of a SPECT system dependent on the rotating camera concept is that a series of planar images are collected while the camera is rotated through either 180o or 36o around the patient. These planar images are called projection images and are used to ;l’’create transaxial slice images by filtered back projection of the data into the transaxial plane. Figure 1.1. is a diagram of such a system with various axes and, in particular, with the axis of rotation indicated and identified . Each row of pixels across the projection image gives a projection line, a profile of counts for a common Y value in that image. The counts in these projection lines may be back projected at the appropriate angle across the transaxial plane, which would result in a first order approximation of the data that gave rise to the set of projection images. (IAEA SERIES NO.6, 2001).

FIG.2. 1 . Diagram of a SPECT system showing the axis of rotation.

2.3. SPECT machine components :

SPECT camera designs are based on a number of fundamental components, all of which play an integral role in the system performance and choice of a SPECT system.

Components of the system:

The two principal components of the system are a conventional scintillation camera system and a computer to which it is interfaced. However, in addition, there will be:

(1) Patient bed (pallet or couch). Tomographic beds are normally specially designed and differ considerably from conventional scintillation camera beds. They are much narrower, so that the camera can rotate with a small radius of rotation. They are made of special material in order to minimize attenuation. They are often designed so that the long axis of the bed can be aligned with the axis of rotation. Finally, the bed height and sometimes the horizontal bed position (shifting the bed laterally) can be controlled either manually or under motorized control. In particular for brain SPECT, there should be a support provided for the patient’s head that permits the radius of rotation to be reduced to a minimum and permits the patient’s head to be tilted at the desired angle.

(2) Gantry. Tomographic gantries are designed to rotate the camera head(s) about the patient. Often, they are mechanically rather massive and in many cases move under the control of a microprocessor interfaced to the main computer. This controller may comprise just a rotation controller or a much more complex system running more or less autonomously.

(3) Rotation controller. This device controls the rotation of the camera around the axis of rotation. It is normally interfaced to the main computer. For a step and shoot system this interface controls the angular increment between successive projection images. For a continuous rotation system, this interface controls the speed of rotation. In addition, it

often permits the camera to be returned to its home position. Such a controller also controls, where appropriate, the lateral position of the gantry and any other mechanical motions under the control of the system. In many cases, on modern systems, the rotation controller not only determines the radius of rotation of a system for all angles, but also the exact position of the head for each individual angle so that various known orbits can be executed.

(4) Emergency stop and other patient safety devices. All tomographic systems have (or should have) an emergency stop button to prevent or abort motion that might injure a patient. Some systems have, in addition, a patient safety device, such as a pressure sensitive pad on the collimator face, that stops motion or automatically moves the detector away from the patient when the system touches the patient couch or the patient.

(5) Position readout devices. These are devices whereby information such as angular position and radius of rotation are displayed. They vary considerably from system to system. In particular, most systems have some method for checking the tilt of the head, e.g. a spirit level attached to the camera head. Such position readout devices should not be relied upon for accuracy, in particular with respect to the centring of the system. (IAEA SERIES NO.6, 2001).

2.3.1. Camera

- Single, dual, triple, or quadruple head large field of view gamma camera.
- Camera(s) positioned as close as possible to body surface without brushing.
- Patient comfort is a consideration. (Pete Shackett et al, 2012).

Single-headed rotating gamma camera systems have been in use for routine SPECT throughout the world for many years but are increasingly being replaced by dual-headed systems. All gamma camera manufacturers now offer SPECT systems as part of their model range. Although all these systems do basically the same thing, namely move the camera head through 360◦ around the patient, there are variations in system design. These variations mainly reflect differences in conventional camera design, in particular how the head is moved and supported.Most SPECT systems were originally modifications of the manufacturer’s basic models but current models have usually been designed with SPECT in mind. Dual-headed and even triple-headed rotating camera systems are now commercially available, their attraction being the increase in sensitivity giving the option of improved image quality and/or shorter imaging times. Dual-headed systems have become particularly popular in recent years as they present a cost-effective alternative to a single-headed system. This is because, although around 50% more expensive in capital costs, they occupy no more space and require no more staff. They, therefore, have the potential to increase patient throughput and/or image quality at little additional revenue cost.

Most systems are now“variable angle” in that the heads can be positioned at various angles relative to each other (Figure 1.2), for example positioning the heads at 90◦ to each other so the benefits of two heads can still be applied to 180◦ acquisition is popular in myocardial perfusion imaging. A number of modifications to the standard rotating gamma camera have resulted from the recent emphasis on cerebral SPECT imaging. Ideally the radius of rotation should be as small as possible and values of around 15 cm can be achieved when imaging the brain. One way of reducing this further is to remove the safety pad from the camera face, although a risk assessment should be carried out before doing this; it may be an option for some patient groups but not for others. In practice the limiting factor is often the patient's shoulders, since it is difficult to avoid these while keeping the patient's head in the field of view, and the radius of rotation can be as large as 25 cm. Since the body outline is closer to an ellipse than a circle, a camera rotating on a circular orbit will be further from the patient than necessary most of the time. Many rotating cameras have the option of a non-circular orbit or of following the patient contour; depending on the camera design, an easier option is often to retain the circular motion of the camera but move the couch during the study to minimize the patient–camera distance. Other systems combine head and couch movement during acquisition. Modifications of this type are probably more relevant to body rather than head imaging, but have been shown to improve resolution. (Peter F et al, 1998).

a

b

Figure 2.2. Dual-headed gamma cameras with the heads at **a** 180◦ for brain imaging and **b** 90◦ for myocardial perfusion imaging.

2.3.2.Detector type:

Detector types include scintillation cameras (i.e., Anger), solid-state, pixilated scintillation crystals, and semiconductor/solid-state detectors.These devices produce either single or multiple transverse sections using one or more rings of focused detectors respectively. In these systems the detectors are usually moved laterally and then rotated to 9produce the profiles used for backprojection.

The advantage of these devices over rotating gamma cameras is improved spatial resolution and increased sensitivity per section. This permits high-quality sections to be obtained in a few minutes, and so dynamic SPECT studies are possible.Most clinical SPECT is, however, carried out on stable distributions of radioactivity, and so this potential advantage has yet to be realized. A weakness of these systems is that the section or sections being imaged have to be selected either fro anatomical landmarks or from a rectilinear scan; this can be a problem and often wastes time. Given that the spatial resolution of the latest SPECT cameras is only slightly poorer than the much more expensive single-section devices, these systems seem likely to be restricted to a few specialist centers. (Peter F et al, 1998).

2.3.3.Energy resolution:

Energy resolution is an important determinant of image quality. The energy window needs to be adjusted for technetium or thallium. It can be improved with solid-state detector technology.

2.3.4.Spatial Resolution:

Spatial resolution is mainly affected by the collimator in Anger camera designs. The image reconstruction algorithm and filtering also affect the final resolution.

2.3.5.Collimators:

The collimator is the most important component of the SPECT system for determining image quality. The width and depth of the collimator septa control the trade-offs between sensitivity and resolution. Low-energy, high-resolution (generally preferred with Tc-99m-based agents) collimators and low-energy, all-purpose (generally preferred for Tl-201) collimators are most commonly used. Parallel hole collimation is most often used in

Anger cameras.The use of newer reconstruction algorithms, the dose and type of radionuclide, the patient population tested, and collimator choice will vary among laboratories.

Collimator

- Matched to radioisotope. Generally, low energy, high resolution or medium energy, general purpose or high resolution.
- Make sure a center of rotation (COR) has been done for the collimators of choice and flood tables loaded for the radioisotope. (Pete Shackett et al, 2012).

2.4. Quality Control of SPECT:

This section will review the most common and useful procedures for modern SPECT systems.

2.4.1.Uniformity

One of the major sources of artifacts in tomographic imaging is non-uniformity in

the flood image. The degree of non-uniformity in the response of a gamma camera to a uniform field of radiation can be defined in terms of the global and local variations in uniformity over the field of view (integral and differential uniformity, respectively) (NEMA, NU 1-1994).

Integral uniformity is defined as the largest variation (maximum - minimum) in counts over the useful field of view, while differential uniformity is a measurement of the worst case rate of change of uniformity over a limited distance (~5 pixels). Modern gamma camera systems typically have integral and differentia uniformities of between 4-7%.

Non-uniformities of this magnitude can generate ring artifacts in tomographic data (Rogers WL et al,1982), hence all tomographic systems apply an additional correction to the raw image data, called "uniformity", "flood" or "sensitivity" correction, before data reconstruction. Following uniformity correction, a tomographic system in good working order will have values of differential uniformity in the range 1.0-2.5%, with values of integral uniformity a little higher at 1.5-3.5%. In order to understand the magnitude and type of non-uniformity that can create a ring artifact, it is necessary to understand the mechanism by which ring artifacts are generated. The reconstruction process assumes that the gamma camera has perfect uniformity. During back-projection, all pixels are assumed to have equal weight and are back-projected with equal intensity. If the counts in one pixel of the image are artificially reduced (e.g. due to a dent in the collimator), then information at that location will be back-projected at that reduced level. The result in the reconstructed image will be a ring artifact, with the radius of the ring equal to the distance of that pixel from the center of rotation (Gullberg GT, 1987). In practice, no system demonstrates perfect uniformity and there will always be minor changes in uniformity from one pixel to the next, even with uniformity correction. Each and every one of these minor changes in uniformity will result in a ring artifact. However, they are only of concern when their magnitude exceeds the noise level in the transaxial image and they can be perceived above image noise. Because ring artifacts are the result of rapid changes in uniformity from one pixel to the next, a parameter that measures changes in uniformity from pixel to pixel will be the most sensitive to the detection of ring artifacts.

Hence measurement of differential uniformity is the most useful indication of the suitability of the system for SPECT. Unfortunately, measurement of differential uniformity is not available on many gamma camera systems and the user must resort to measurement of integral uniformity in its place. How good (or low) the values of differential uniformity must be to ensure the absence of ring artifacts in clinical studies depends on the clinical study. The purpose of uniformity correction is to reduce system non-uniformities to a low enough level so that any ring artifacts generated from residual non-uniformities in the system are less than image noise and hence are not visible in the reconstructed data. However, image noise in the reconstructed data will vary significantly with the type of study, hence a low count In-111 SPECT study will be far noisier than a high count Tc-99m liver SPECT study.

Therefore a ring artifact that may be clearly visible in the Tc-99m liver SPECT study, may not be visible in the In-111 SPECT study. This implies that greater non-uniformities can be tolerated for some types of clinical studies than for others (O'Connor MK et al, 1991). Rather than estimating the level of system uniformity required for different types of studies, it is simpler to correct system non-uniformities to a level that will ensure no visible ring artifacts in even the highest count clinical studies. In general, it has been found that a 30 million count flood image provides sufficiently good correction of system non- uniformities for all current clinical studies. This correction should result in a value for differential uniformity of less than 3% (O'Connor MK et al, 1991). It should be noted that this level of correction might not be adequate for some types of phantom studies. For example, a Jaszczak phantom with 10mCi Tc-99m may give 50-70 million counts over a

30 minute SPECT acquisition, and in such studies ring artifacts may be noted even though the system uniformity is adequate for clinical studies.

For routine QC of a SPECT system it is necessary to quantitate the degree of non-uniformity in the system. In order to obtain adequate counting statistics, significantly more counts must be acquired in the flood image compared to what is acquired for planar QC. Practical considerations usually limit the number of counts in the uniformity image to between 5-10 Mcts. With total counts less than 5 Mct, measurements of integral and differential uniformity are significantly altered by image noise (Young KC et al, 1990). The values for differential uniformity should be tracked on a daily basis and action taken (e.g. acquire a new uniformity correction map) when the values exceed 3-4%.

2.4.2. Center of Rotation

Accurate center of rotation (COR) correction is important for high quality tomography. Errors in COR of as little as 0.5 pixel in a 128 x 128 matrix can lead to degradation in image quality (Cerquira MD et al, 1988). COR is measured by performing a 360 degree acquisition around a point source of Tc-99m. Most manufacturer's have software designed to analyze the acquisition and determine if the COR is within acceptable limits. Not only is it important to use the correct value of COR, it is also essential that this value remain constant as a function of angle. When measured on a gamma camera system, at a radius of rotation of 20 cm, both the X and Y values for the COR should show less than a 2 mm variation over a 360oorbit. COR is normally a very stable parameter of modern gamma camera systems and a weekly check is adequate to ensure proper correction.

2.4.3.Tomographic Resolution

An overall assessment of system performance can be obtained by imaging a suitable tomographic phantom. These are usually circular phantoms containing a variety of rods or spheres that can be filled with a mixture of water and Tc-99m. The usual purpose of this phantom is to determine optimum system performance. Hence the phantom is imaged under ideal conditions, i.e. minimum radius of rotation, high resolution collimation, 128 x 128 matrix with at least 120 views and high total counts (30-50 Mcts). The phantom should be placed on the headrest of the imaging table.

Reconstruct transaxial images of the phantom with minimum smoothing. Single pixel thick slices through the uniform section of the phantom can be used to evaluate uniformity. Thicker slices through the resolution elements can be used to determine tomographic resolution. Note that because of the high counts present in such an acquisition, it is often necessary to acquire a high-count uniformity correction map (~100 Mcts or more) in order to provide adequate uniformity correction for this study. This test of tomographic resolution and uniformity should be performed every 6 months.

2.4.4.Rotational Uniformity

On most SPECT systems, the "uniformity" correction map is generated from a flood image acquired with the detector head facing up. It is then assumed that this correction map can be applied to images acquired at all angles of rotation. There are a number of instances when this assumption may not be valid. The photomultiplier tubes within the detector head are heat sensitive; hence heat generated by the electronics within the head may alter their characteristics. If the heat distribution within the head changes as a function of angle, then so too can the performance characteristics of the detector. Another likely cause of variations in uniformity with angle of rotation, is poor optical coupling of a PMT to the light guide or crystal. This can cause the tubes to decouple slightly at certain angles, leading to a significant change in uniformity. Photomultiplier tubes are also sensitive to the earth's magnetic field. Their performance characteristics can change with their orientation to the earth's magnetic field, leading to changes in uniformity with rotation (Rogers WL et al, 1982). This may be a problem in older SPECT systems with inadequate magnetic shielding. A simple test for the assessment of rotational uniformity is to securely tape a lightweight Co-57 sheet source to the collimator face and perform a high-count tomographic acquisition over 360o. In order to obtain sufficient counts, this acquisition can take several hours and is often best performed overnight. The raw data can then be played back in cine mode to check for significant changes in uniformity with rotation. Note: many modern systems have pressure sensitive cover plates on the collimator face. In such cases, this test can only be performed if this feature of the system can be bypassed. Measurement of rotational uniformity should be performed once or twice a year, or whenever a significant upgrade or repair has been made to the detector head.

2.4.5.Collimator hole-alignment

Parallel-hole collimators are assumed to have the orientation of the holes perpendicular to the surface of the crystal. In reality there can be considerable variation in collimator hole angle both locally and globally. These variations directly affect the center of rotation and a poorly manufactured collimator may have considerable variations in COR across its surface. These variations cannot be corrected for by the standard COR correction method, and their presence cannot be determined by inspection of planar image quality. While such collimators will often produce acceptable planar images, the quality of SPECT images will be inferior. Unfortunately the only solution for this type of problem is replacement of the collimator. A simple way to check a collimator is to perform multiple measurements of COR along the length of the collimator, and check that all measurements essentially give the same result (Cerquira MD et al, 1988). Maximum variations in COR should not exceed + 1.0 mm over the length of the collimator Busemann-Sokole E, 1987), (Malmin R et al, 1990). Larger variations than this indicate local hole angulation errors. Furthermore, the average COR value for the collimator should be similar to those for the other collimators on the tomographic system. Measurement of collimator hole alignment need only be performed once for each collimator, as it is solely a function of the physical characteristics of the collimator.

2.4.6.Gantry alignment (single head system)

For a tomographic acquisition in single headed SPECT systems, the gantry is usually set to 0o and the detector head is leveled prior to an acquisition. Setting the detector head level is based on the assumption that the axis of rotation of the detector head is horizontal. This axis of rotation is determined by the alignment of the gantry. Misalignment of the gantry can be caused by a number of things. In many older SPECT systems, sagging of the detector arms can occur. This is particularly true in cantilevered systems as compared with counterbalanced systems. The gantry itself may not be level on the floor, either due to incorrect shimming of the gantry, or irregularities in the surface of the floor. Whatever the cause, the consequences are that leveling the detector head results in data being acquired obliquely rather than perpendicular to the axis of rotation. For example, a 1ogantry misalignment with the detector head at a 20 cm radius of rotation will cause a 3.5 mm displacement of image data along the axis of rotation. Variations in gantry alignment will be visible in the analysis of the weekly COR measurement as variations in the Y-position of the point source. Gantry alignment and its stability with rotation can also be easily checked using a small bubble level. Level the gantry ato, then rotate the gantry through 180o and check that the gantry is still level. Alignment should be checked once or twice a year and after any major upgrade or modification to the gantry.

2.4.7.Head alignment (multi-head systems)

Many multi-detector systems do not permit tilting of the detector head and hence if the gantry is not vertical, it is not possible to level the head and misalign the detector relative to the gantry. However a new concern with multi-detector systems is the alignment of a given detector to itself at different radial positions and the alignment between the different detectors. A simple method of simultaneously checking radial alignment, inter-head alignment and collimator hole alignment is to acquire tomographic acquisitions of a point source. Assuming that we are evaluating a dual-head 90o system, and then the following two acquisitions need to be performed. With the point source located close to the center of rotation of the gantry, acquire a 360o acquisition of the point source with head #1 at the minimum radius of rotation. Now acquire a second acquisition with head #2 at the maximum radius of rotation. Reconstruct both studies in an identical manner. The only difference between the two sets of transaxial images is the loss of resolution in head #2 data due to the increased distance from the point source. Now subtract the transaxial images from the head #1 from those of head #2. If there is no misalignment, the resulting images should show a doughnut shape indicating perfect co-registration of the two heads. Any misalignment of the two heads will be readily apparent on the subtracted images. This is a very simple but useful test that will work on dual-head 90o systems, as well as conventional dual-head and triple-head systems.

This test need only be performed on a 6-month or yearly basis. It should be repeated if any changes in COR are noted in the weekly QC.

2.4.8. Fan-Beam Collimators

Fan-beam collimators are coming into widespread use for brain and cardiac studies. The cause of artifacts associated with this type of collimator is often difficult to determine, as the raw data is in a distorted form and difficult to interpret. The primary factor of interest with a fan-beam collimator is focal length. A number of techniques have been described that allow the user to determine both the true focal length of the collimator and an estimate of the variation in this focal length over the collimator field of view [15,16]. The main disadvantage of these techniques is that they require either special software or multiple acquisitions and reconstruction of point sources at different radii of rotation and collimator focal lengths. Fortunately, this process need only be performed once on each collimator to accurately characterize it.

Chapter Three

Materials and Methods

3.1. Materials:

3.1.1. Instrumentations

- SPECT machine:

The data collected from SPECT machine which is known as Symba manufactured by Siemens.

- Personal Computer (PC) , with Intel Pentium IV at 3 GHz (3i Core) , 10 GB RAM , 500GB HDD , 32 x CD-DVD Drive , OS MS – Windows 9x and Printer

- Digitizer scanner

- MatLab version R2009a (7.83.2.3) program

- SPSS version 13

3.2. Study Duration:

This study proposed to be carried between November 2014 to March 2015.

3.3. Study Place:

The proposed study was conducted in College of Medical Radiological Science, Sudan University of Science and Technology.

3.4. Methods:

3.4.1. Methods of data collection: Image enhancement technique:

1.Contrast-limited adaptive histogram equalization (CLAHE):

This technique used to enhance the contrast of the grayscale image by transforming the values using contrast-limited adaptive histogram equalization (CLAHE). CLAHE operated on small regions in the image, called tiles, rather than the entire image, each tile's contrast was enhanced, so that the histogram of the output region approximately matches the histogram specified by the 'Distribution' parameter. The neighboring tiles were then combined using bilinear interpolation to eliminate artificially induced boundaries. The contrast, especially in homogeneous areas, could be limited to avoid amplifying any noise that might be present in the image.

J = adapthisteq(I) enhanced the contrast of the grayscale image I by transforming the values using contrast-limited adaptive histogram equalization (CLAHE).

2.Enhance contrast using histogram equalization:

This programming code (histeq) enhanced the contrast of images by transforming the values in an intensity image, or the values in the colormap of an indexed image, so that the histogram of the output image approximately matched a specified histogram. J = histeq(I, hgram) transformed the intensity image I so that the histogram of the output intensity image J with length(hgram) bins approximately matches hgram. The vector hgram should contain integer counts for equally spaced bins with intensity values in the appropriate range: [0, 1] for images of class double, [0, 255] for images of class uint8, and [0, 65535] for images of class uint16. histeq automatically scales hgram so that sum(hgram) = prod(size(I)). The histogram of J was better match hgram when length (hgram) is much smaller than the number of discrete levels in I. J = histeq(I, n) transformed the intensity image I, returning in J an intensity image with n discrete gray levels. A roughly equal number of pixels were mapped to each of the n levels in J, so that the histogram of J is approximately flat. (The histogram of J was flatter when n was much smaller than the number of discrete levels in I) The default value for n is 64. [J, T] = histeq(I,...) returned the grayscale transformation that maps gray levels in the image I to gray levels in J. newmap = histeq(X, map, hgram) transformed the colormap associated with the indexed image X so that the histogram of the gray component of the indexed image (X,newmap) approximately matches hgram. The histeq function returns the transformed colormap in newmap. length(hgram) must be the same as size(map,1). newmap = histeq(X, map) transformed the values in the colormap so that the histogram of the gray component of the indexed image X is approximately flat. It returns the transformed colormap in newmap. [newmap, T] = histeq(X,...) returned the grayscale transformation T that maps the gray component of map to the gray component of newmap.

3.**Adjust image intensity values or colormap:**

This programming code (imadjust) used to enhance the images by increased of contract of the image , J = imadjust(I) mapped the intensity values in grayscale image I to new values in J such that 1% of data is saturated at low and high intensities of I. This increased the contrast of the output image J. This syntax was equivalent to imadjust(I,stretchlim(I)). J = imadjust(I,[low_in; high_in],[low_out; high_out]) maps the values in I to new values in J such that values between low_in and high_in map to values between low_out and high_out. Values below low_in and above high_in were clipped; that is, values below low_in map to low_out, and those above high_in map to high_out. Could use an empty matrix ([]) for [low_in high_in] or for [low_out high_out] to specify the default of [0 1]. J = imadjust(I,[low_in; high_in],[low_out; high_out],gamma) maps the values in I to new values in J, where gamma specifies the shape of the curve describing the relationship between the values in I and J. If gamma was less than 1, the mapping was weighted toward higher (brighter) output values. If gamma was greater than 1, the mapping was weighted toward lower (darker) output values. If omitted the argument, gamma defaults to 1(linear mapping). newmap = imadjust(map,[low_in; high_in], [low_out; high_out],gamma) transforms the colormap associated with an indexed image. If low_in, high_in, low_out, high_out, and gamma were scalars, then the same mapping applies to red, green, and blue components. Unique mappings for each color component are possible when low_in and high_in are both 1-by-3 vectors. low_out and high_out are both 1-by-3 vectors, or gamma was a 1-by-3 vector. The rescaled colormap newmap was the same size as map. RGB2 = imadjust(RGB1,...) performs the adjustment on each image plane (red, green, and blue) of the RGB image RGB1. As with the colormap adjustment, could apply unique mappings to each plane.

4. 2-D median filtering:

Median filtering was a nonlinear operation often used in image processing to reduce "salt and pepper" noise from the images . A median filter was more effective than convolution when the goal was to simultaneously reduce noise and preserve edges. B = medfilt2(A, [m n]) performs median filtering of the matrix A in two dimensions. Each output pixel contains the median value in the m-by-n neighborhood around the corresponding pixel in the input image. medfilt2 pads the image with 0s on the edges, so the median values for the points within [m n]/2 of the edges might appear distorted. B = medfilt2(A) performs median filtering of the matrix A using the default 3-by-3 neighborhood. B = medfilt2(A, 'indexed', ...) processes A as an indexed image, padding with 0s if the class of A is uint8, or 1s if the class of A is double. B = medfilt2(..., padopt) controls how the matrix boundaries were padded. padopt may be 'zeros' (the default), 'symmetric', or 'indexed'. If padopt is 'symmetric', A was symmetrically extended at the boundaries. If padopt is 'indexed', A was padded with ones if it was double; otherwise it was padded with zeros.

5. 2-D order-statistic filtering:

This programming code used to enhance of the images. B = ordfilt2(A, order, domain) replaced each element in A by the orderth element in the sorted set of neighbors specified by the nonzero elements in domain. B = ordfilt2(A, order, domain, S) where S was the same size as domain, useed the values of S corresponding to the nonzero values of domain as additive offsets. B = ordfilt2(..., padopt) controls how the matrix boundaries were padded. Set padopt to 'zeros' (the default) or 'symmetric'. If padopt was 'zeros', A was padded with 0's at the boundaries. If padopt was 'symmetric', A was symmetrically extended at the boundaries.

6. contrast stretch image:

This programming code used to enhance of the images , LOW_HIGH = stretchlim(I) returns LOW_HIGH, a two-element vector of pixel values that specify lower and upper limits that can be used for contrast stretching image I. By default, values in LOW_HIGH specify the bottom 1% and the top 1% of all pixel values. The gray values returned can be used by the imadjust function to increase the contrast of an image. LOW_HIGH = stretchlim(I, TOL) where TOL is a two-element vector [LOW_FRACT HIGH_FRACT] that specifies the fraction of the image to saturate at low and high pixel values. If TOL is a scalar, LOW_FRACT = TOL, and HIGH_FRACT = 1 - LOW_FRACT, which saturates equal fractions at low and high pixel values. If you omit the argument, TOL defaults to [0.01 0.99], saturating 2%. If TOL = 0, LOW_HIGH = [min(I(:)); max(I(:))]. LOW_HIGH = stretchlim(RGB, TOL) returns a 2-by-3 matrix of intensity pairs to saturate each plane of the RGB image. TOL specifies the same fractions of saturation for each plane.

3.4.2.Method of data Analysis:

The data analyzed by using statistical package, Statistical Package for Social Studies (SPSS) under windows.

3.4.3. Methods of data storage:

The data stored securely in password Personal computer (PC)

3.5. Ethical issues:

- No patient data will be published

Chapter Four

The Results

Figure 4-1. The original image test (A1)

Figure 4-2. CLAHE technique; at upper side the original image with histogram and at lower side the enhanced image using CLAHE technique from test (A1)

Figure 4-3. The original image test (A2)

Figure 4-4. histogram equalization technique; at upper side the original image with histogram and

at r side the enhanced image using histogram equalization technique from test (A2)

Figure 4-5. The original image test(A3)

Figure 4-6. Adjust technique; at upper side the original image with histogram and at lower side the enhanced image using Adjust technique from test (A3)

Figure 4-7. The original image test (A4)

Figure 4-8. 2-D median filtering technique; at upper side the blurring image with histogram and at lower side the enhanced image using 2-D median filtering technique from test (A4)

Figure 4-9. The original image test (A5)

Figure 4-10. 2-D order-statistic filtering technique; at upeer side the original image with histogram and at lower side the enhanced image using 2-D order-statistic filtering technique from test (A5)

Figure 4-11. The original image test (A6)

Figure 4-12. Contrast stretch image technique; at upeer side the original image with histogram and at lower side the enhanced image using contrast stretch image technique from test (A6)

Figure 4-13. The original image test (B1)

Figure 4-14. CLAHE technique; at upper side the original image with histogram and at lower side the enhanced image using CLAHE technique from test (B1).

Figure 4-15. The original image test (B2)

Figure 4-16. histogram equalization technique; at upper side the original image with histogram and at r side the enhanced image using histogram equalization technique from test (B2)

Figure 4-17. The original image test(B3)

Figure 4-18. Adjust technique; at upper side the original image with histogram and at lower side the enhanced image using Adjust technique from test (B3)

Figure 4-19. The original image test (B4)

Figure 4-20. 2-D median filtering technique; at upper side the blurring image with histogram and at lower side the enhanced image using 2-D median filtering technique from test (B4)

Figure 4-21. The original image test (B5)

Figure 4-22. 2-D order-statistic filtering technique; at upeer side the original image with histogram and at lower side the enhanced image using 2-D order-statistic filtering technique from test (B5)

Figure 4-23. The original image test (B6)

Figure 4-24. Contrast stretch image technique; at upeer side the original image with histogram and at lower side the enhanced image using contrast stretch image technique from test (B6)

Chapter Five:

Discussion, Conclusion and Recommendations

5.1. Discussion:

Nuclear medicine images show characteristic information about the physiological properties of the structures-organs. In order to have high quality medical images for reliable diagnosis, the processing of image is necessary. The scope of image processing and analysis applied to medical applications is to improve the quality of the acquired image and extract quantitative information from medical image data in an efficient and accurate way. In Nuclear Medicine, there are two main methods of patient imaging, the imaging with Planar Imaging, Dynamic Imaging or SPECT and the PET. In this study data analyzed by using MatLab program to enhance the contrast within the images, the gray levels in both enhanced and unenhanced images and noise variance. The technique used for this study were Contrast-limited adaptive histogram equalization (CLAHE) which operated on small regions in the image, called tiles, rather than the entire image, each tile's contrast was enhanced, so that the histogram of the output region approximately matches the histogram specified by the 'Distribution' parameter., Enhance contrast using so that the histogram of the output region approximately matches the histogram specified by the 'Distribution' parameter. The neighboring tiles were then combined using bilinear interpolation to eliminate artificially induced boundaries. The contrast, especially in homogeneous areas, could be limited to avoid amplifying any noise that might be present in the image as shown in figure 4-2 and figure 4-15. The histogram equalization enhanced the contrast of images by transforming the values in an intensity image, or the values in the colormap of an indexed image, so that the histogram of the output image approximately matched a specified histogram as shown in figure 4-4 and figure 4-17. Adjust image intensity values or colormap used to enhance the images by increased of contract of the image, it mapped the intensity values in grayscale image as shown in original image (figure 4-1) to new values in figure 4-6 and figure 4-19 such that 1% of data is saturated at low and high intensities of I. 2-D median filtering used as nonlinear operation which often used in image processing to reduce "salt and pepper" noise in figure 4-8 and figure 4-21 from the images as in figure 4-9 and figure 4-22. A median filter was more effective than convolution when the goal was to simultaneously reduce noise and preserve edges. 2-D Order-Statistic filtering used to enhance of the images.replaced each element by the orderth element in the sorted set of neighbors specified by the nonzero elements in domain as in figure 4-11 and figure 4-24 . Contrast stretch image used to enhance of the images within which a two-element vector of pixel values that specify lower and upper limits that can be used for contrast stretching image as in figure 4-13 and figure 4-20. The results of this technique agreed the results of Robiul et al, (2011), Nasrul et al, (2012), Gupta et al, (2012) and Smriti et al, (2012) who used non-linear filtering based methods to enhance the nuclear medicine images. The anther technique was Convolution kernel filter. Filtering is a technique for modifying or enhancing an image. For example, researchers can filter an image to emphasize certain features or remove other features. Image processing operations implemented with filtering include smoothing, sharpening, and edge enhancement. Filtering is a neighborhood operation, in which the value of any given pixel in the output image is determined by applying some algorithm to the values of the pixels in the neighborhood of the corresponding input pixel. A pixel's neighborhood is some set of pixels, defined by their locations relative to that pixel. Linear filtering is filtering in which the value of an output pixel is a linear combination of the values of the pixels in the input pixel's neighborhood.

5.2. Conclusion:

- The quality of images is increased by using Matlab techniques.
- The very small detail's of the image could be clearly appear at used this techniques
- The sensitivity is increased in this study.
- The histogram is appear the significant different of enhance the images.
- Used non-linear filtering based methods to enhance the nuclear medicine images by

reduce of "salt and pepper" noise.

- Implemented the image processing operations with filtering to smoothing, sharpening and edge enhancement.

5.3.Recommendations:

- Image enhancement is basically improving the interpretability or perception of information in images , it,s important to develop image enhancement programm.
- enhancement algorithms play a critical role in choosing an algorithm for real-time applications. Despite the effectiveness of each of these algorithms when applied separately, in practice one has to devise a combination of such methods to achieve more effective image enhancement.
- Use image enhancement techniques as pre-processing tools for other image processing techniques, then quantitative measures can determine which techniques are most appropriate Spatial domain methods or frequency domain methods .

.

5.4. References:

Busemann-Sokole E: Measurement of collimator hole angulation and camera head tilt for slant and parallel hole collimators used in SPECT. J Nucl Med 1987; 28:1592-1598.

Cerquira MD., Matsuoka D, Ritchie JL, et al: The influence of collimators onSPECT Center of Rotation measurements: artifact generation and acceptancetesting. J Nucl Med 1988; 29: 1393-1397.

Gullberg GT: An analytical approach to quantify uniformity artifacts for circularand noncircular detector motion in single photon emission computed tomographicimaging. Med Phys 1987; 14: 105-114.

IAEA HUMAN HEALTH SERIES NO.6 Quality Assuance for SPECT systems .

Liu J, Loncaric S, Huang G, Chang W. The focussing quality of commercial fan-beam collimators. J Nucl Med 1996; 37: 207P.

Mahowald JL, Robins PD, O’Connor, MK. The evaluation and calibration of fan-beam collimators. Eur J Nucl Med 1999; 26: 314-319.

Malmin R, Stanley P, Guth WR: Collimator angulation error and its effect on SPECT. J Nucl Med 1990; 31:655-659.

NEMA. Performance measurements of scintillation cameras. Washington DC.National Electrical Manufacturers Association (NEMA), 1994, StandardsPublication NU 1-1994

O’Connor MK, Vermeersch C: Critical examination of the uniformityrequirements for single-photon emission computed tomography. Med Phys 1991;18:190-197.

Peter F.Sharp ,Howard G.Gemmell ,Alison D.Murray Editor Practical Nuclear Medicine –Third Edition –1998.

Pete Shackett ,Nuclear Medicine Technology Procedures and Quick Reference-Second Edition -2012.

Rogers WL, Clinthorne NH, Harkness BA, et al : Field flood requirements foremission computed tomography with an Anger camera. J Nucl Med 1982; 23:162-168.

Young KC, Kouris K, Awdeh M, Abdel-Dayem HM. Reproducibility and action levels for gamma camera uniformity. Nucl Med Commun 1990; 11: 95-101.